NMR Solution Structure and Flexibility of a Peptide Antigen Representing the Receptor Binding Domain of *Pseudomonas aeruginosa*[†,‡]

Campbell McInnes, Frank D. Sönnichsen, Cyril M. Kay, Robert S. Hodges, and Brian D. Sykes*

Protein Engineering Network of Centres of Excellence and Synthetic Peptides Incorporated, 713 Heritage Medical Research Building, University of Alberta, Edmonton, Alberta, T6G 2S2, Canada

Received May 18, 1993; Revised Manuscript Received July 27, 1993[⊕]

ABSTRACT: A synthetic peptide antigen corresponding to the C-terminus of *Pseudomonas aeruginosa* K strain pilin has been studied by one and two-dimensional NMR techniques. This peptide exists in two isomeric forms which arise as a result of the I^{138}–P^{139} amide bond. An ensemble of solution conformations for the *trans* form of this 17-residue disulfide-bridged peptide (PAK 128–144) has been generated using a simulated annealing procedure in conjunction with distance and torsion angle restraints derived from NMR data. One major class of backbone conformations has been identified for this potential synthetic vaccine and indicates the presence of two β-turns in the region 134–142. The region that has been established as the epitope for the monoclonal antibody PK99H is consistent with the region of the major conformers that exhibit the most definition in the ensemble (134–140) and also includes a type I β-turn from residues 134 to 137. The generated structures are also consistent with observed NOEs characteristic of β-turns and amide proton temperature coefficient data, which indicate the presence of two turns between residues 134 and 142. The presence of secondary structure within the epitope substantiates the theory that immunogenic regions of proteins are those which contain surface-exposed structural elements such as β-turns. Further implications of the structure on antigenicity and cross-reactivity are discussed.

Pseudomonas aeruginosa is an opportunistic pathogen which causes often fatal infections in intensive care and cystic fibrosis patients (Rivera & Nicotra, 1982). The first step in the infection process is believed to be attachment to the host cell via pili on the surface of the bacterium (Pier, 1985; Irvin et al., 1990; Irvin, 1993). The pilus of *P. aeruginosa* is composed of a 13–17-kDa monomeric protein subunit called pilin. The C-terminal region of the pilin monomer contains the epithelial cell binding domain (Paranchych et al., 1986; Irvin et al., 1989) and is semiconserved in the seven different strains of this bacterium (Pasloske et al., 1988; Paranchych et al., 1990). A vaccine which generates antisera specific for the C-terminal region of the pilus and thus blocks bacterial attachment to the host cell receptor should be effective in counteracting *P. aeruginosa* infections. Since there is a degree of sequence homology in the C-terminal region and all strains have been shown to bind to the same cell surface receptor (Ramphal et al., 1984), it should be possible to produce a cross-reactive antiserum which inhibits the adherence of all known strains of *P. aeruginosa*.

Monoclonal antibodies have been raised to whole pili which are effective against single strains (Doig et al., 1990; Paranchych et al., 1993), and in some cases cross-react with other strains (Lee et al., 1990). In order to develop a broad spectrum vaccine, it would be expedient to understand the factors which contribute to the strain specificity and cross-reactivity of antibodies specific for the C-terminal region. In understanding the process of antibody–antigen recognition, it is important to determine the conformations of antigenic peptides when free in solution and when bound to their corresponding monoclonal antibody. Determination of the 3D structures of peptides from the pilin C-terminal region of different strains of *P. aeruginosa* should allow a greater understanding of cross-reactivity and facilitate the development of an effective antiadhesion vaccine.

Several investigations into the conformation of peptide antigens have been undertaken at present, mainly employing NMR[1] and X-ray crystallography. The results of these studies show that many immunogenic peptides have a propensity to adopt well-defined secondary structure in aqueous solution (Dyson et al., 1985, 1988a,b; Chandrasekhar et al., 1991; Zvi et al., 1992; Blumenstein et al., 1992). The majority of these peptide antigens exist with a significant population of β-turn conformations. Two investigations of antibody-bound peptides (Sherf et al., 1992; Stanfield et al., 1990) indicate that the residues in the epitope region of the bound peptide form a β-turn in the antibody combining site. These studies suggest that β-turns may comprise a structural motif for antigenic regions of peptides and proteins. Indeed, β-turns generally constitute more than 50% of the surface-exposed regions in globular proteins (Kuntz, 1972) and thus are likely to be immunogenic in nature.

This article presents the structural study of the C-terminal region of the *P. aeruginosa* pilin strain K. A 17-residue peptide from this region representing residues 128–144, KCTSDQD-EQFIPKGCSK, has been studied by ^{1}H NMR and found to exist as two conformations in solution (McInnes et al., 1993). These have been attributed to the *cis/trans* isomerization of the I^{138}–P^{139} amide bond. A set of interproton distances and torsion angles obtained for the *trans* conformer using 2D NMR data sets has been used to generate an ensemble of possible conformations. The 3D structures show the presence of two

† This research is a contribution from the Protein Engineering Network of Centres of Excellence, which is funded by the Government of Canada. C.M. is supported by a P.E.N.C.E. postdoctoral fellowship.

* Author to whom correspondence should be addressed.

‡ Data can be accessed from the Protein Data Bank under filenames 1PAJ and 1PAK.

⊕ Abstract published in *Advance ACS Abstracts,* November 1, 1993.

[1] Abbreviations: CD, circular dichroism; DQF-COSY, double quantum filtered correlated spectroscopy; HPLC, high-performance liquid chromatography; NMR, nuclear magnetic resonance; NOE, nuclear Overhauser enhancement; NOESY, nuclear Overhauser enhancement spectroscopy; PAK, *Pseudomonas aeruginosa* K strain; rmsd, root-mean-square deviation; SA, simulated annealing; TOCSY, total correlation spectroscopy.

0006-2960/93/0432-13432$04.00/0

β-turns encompassing residues 134–137 and 139–142. The β-turn between residues 134 and 137 is part of the epitope region for the monoclonal antibody PK99H generated against whole pili strain PAK and, thus, is consistent with the previously mentioned investigations of immunogenic peptides. Further discussion of the 3D structure of PAK 128–144 and its immunological significance is presented here.

EXPERIMENTAL PROCEDURES

Peptide Synthesis. Ac-KCTSDQDEQFIPKGCSK-OH, corresponding to the region 128–144 of the *P. aeruginosa* K strain pilin, was synthesized and purified by solid-phase synthesis and reversed-phase HPLC, respectively, as reported by Wong et al. (1992). This peptide was studied in its oxidized form with the disulfide bridge between C^{129} and C^{142}.

NMR Sample Preparation. PAK 128–144 was dissolved in 500 μL of 90% H_2O/10% D_2O containing 100 mM KCl and 20 mM NaAc to a concentration of 5 mM. 2,2-Dimethyl-2-sila-5-pentanesulfonate (DSS) was added as an internal chemical shift reference, and the pH was adjusted to 5 using small aliquots of NaOD and DCl solutions.

NMR Spectroscopy. The observed nucleus in all experiments was ^1H. Spectra were measured at 600 MHz utilizing a Varian Unity 600 spectrometer. One- and two-dimensional experiments were performed at 5.0, 10.0, 15.0, 20.0, and 25.0 °C using presaturation to accomplish suppression of the water resonance. Two-dimensional experiments were acquired by the hypercomplex method (States et al., 1982), typically using 32 transients for each of 300 increments. Proton resonances were assigned as reported (McInnes et al., 1993) using TOCSY (Bax & Davis, 1985), NOESY (Jeener et al., 1979), and DQF-COSY (Piantini et al., 1982) spectra, each employing a spectral width of 8000 Hz and 2048 data points. NOESY experiments were performed at 75, 100, 125, 150, 175, 200, 250, 300, 350, and 400 ms in order to assess the NOE buildup profile of the peptide. Gaussian processing with resolution enhancement was used for NOESY and TOCSY spectra, while shifted sine bell apodization was utilized during transformation of the DQF-COSY.

Circular Dichroism Spectroscopy. CD experiments were performed on a Jasco J720 spectropolarimeter (Jasco Inc., Easton, MD) interfaced to an Epson Equity 386/25 and controlled by Jasco software. The cell holder temperature was maintained at 24.7 °C using a Lauda RMS circulating water bath (Lauda, Westbury, NY). The instrument was routinely calibrated with ammonium *d*-(+)-camphorsulfonate at 290.5 and 192 nm. The sample was prepared by dissolving PAK 128–144 to a concentration of 1.14 mg/mL in 0.1 M KCl and adjusting the pH to 7.0. The sample was placed in a cell with path length 0.01 cm and the spectra recorded between 182 and 255 nm, employing 10 scans and noise reduction to remove the high frequency. The voltage of the photomultiplier was kept below 500 V to prevent distortion of the CD spectrum. The CD spectra were analyzed using the Contin program (Provencher & Glöckner, 1981).

Data Analysis. Interproton distances for PAK 128–144 *trans* were obtained by integrating all cross-peaks from the NOESY spectrum acquired at 5.0 °C with a 200-ms mixing time. The integral volumes were then converted to distance restraints using a reference distance of 2.55 Å for the β to δ protons of F^{137}. The restraint file was generated using a program, written by R. Boyko and F. Sönnichsen of the University of Alberta, which utilizes the cross-peak intensity and assignment files and groups them into the requisite number of classes. The categories used were strong (upper boundary, 2.7 Å), medium (upper boundary, 3.3 Å), and weak (upper boundary, 5.0 Å). A total of 181 distance restraints was generated using this method.

$^3J_{NH\alpha CH}$ coupling constant information was obtained from the DQF-COSY acquired at 5.0 °C, processed using sine bell weighting, and zero filled to 16K × 2K. Traces for resolved cross-peaks were taken in F2 and then curve-fitted using a program, written by R. Boyko and F. Sönnichsen of the University of Alberta, which utilizes an iterative fitting procedure. Torsion angle restraints were generated using the Stereosearch program (Nilges et al., 1990), which requires $^3J_{NH\alpha CH}$ coupling constant and sequential NOE information as input. A total of 14 possible dihedral ϕ and φ restraints was generated by this program. An additional 20° was subtracted from the lower boundary and added to the upper boundary in order to account for inaccuracies. Two generic distance restraints were used corresponding to the hydrogen bonds between the D^{134} carbonyl and F^{137} NH and the P^{139} carbonyl and C^{142} NH, and were set at 3.0 Å.

3D Structure Calculations. Structural calculations were performed using Biosym software (San Diego, CA). These employed the simulated annealing (SA) protocol within the Insight II user interface. The simulated annealing program (Nilges et al., 1988) as a means of 3D structure determination searches for the global minimum of a target function (comprising the standard energy terms of the CVFF force field for bonded interactions and a simple quartic nonbonded potential with van der Waals radii scaled by 0.85) by substantially reducing the force constants and then selectively scaling these up until the full values are regained. The distance information was included using a skewed biharmonic potential which was equal for all restraints. All peptide bonds were forced to *trans* geometry during the calculations. Charge interactions and cross-terms were not included in the calculations. A cutoff distance of 5 Å was used.

The restrained simulated annealing procedure used consists of 14 stages. These include an initial energy minimization of randomly distributed atoms (100 steps steepest descent and 2000 steps conjugate gradient). This was followed by 55 ps of molecular dynamics in three stages at 1000 K, during which the NOE force constants were scaled from 0.000 01 to 20 kcal, 10 ps of molecular dynamics during cooling to 300 K in five stages, and a final full energy minimization in four stages (100 steps steepest descent, 2000 steps conjugate gradient, 100 steps steepest descent, and 15 000 steps conjugate gradient). A total of 12 SA runs was performed with the final run incorporating an NOE force constant twice that used in previous runs. All restraints used were weighted equally in all structures in each of the SA runs. The average structure was calculated from the final run, and rmsd comparisons were made using programs written by T. Jellard of the University of Alberta.

RESULTS

Distance Restraints. ^1H NMR experiments on oxidized PAK 128–144 have shown it to exist as two distinct conformations in solution attributable to *cis/trans* isomerization of the I^{138}–P^{139} amide bond (McInnes et al., 1993). The proton resonance assignments, $^3J_{NH\alpha CH}$ values, and amide temperature coefficients for both isoforms have been reported and indicate that the two forms differ significantly in their 3D structures (McInnes et al., 1993). Through the use of resonance assignments, all cross-peaks from the NOESY spectrum of PAK 128–144 acquired at 5.0 °C with a mixing time of 300 ms were labeled for both the *cis* and *trans* isoforms.

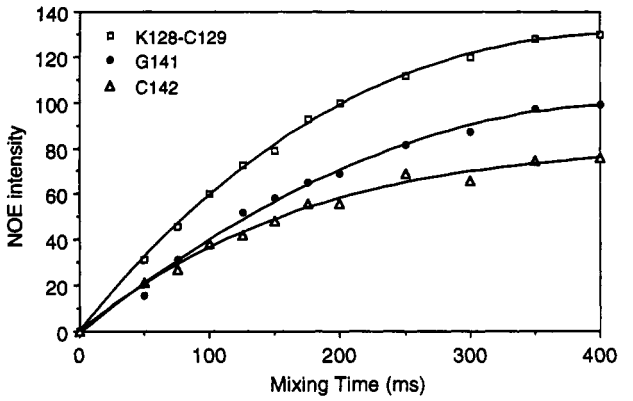

FIGURE 1: NOE buildup rates for selected $d_{\alpha N}$ cross-peaks from the 600-MHz NOESY spectrum of oxidized 5 mM PAK 128–144 in 90% H_2O/10% D_2O (pH 5), 20 mM NaAc, and 100 mM KCl at 5.0 °C.

A total of 273 cross-peaks was assigned for both isomers, of which 184 were attributed to the *trans* form and 89 to the *cis* form. Of the 89 NOEs associated with the *cis* isomer, a limited number corresponded to interresidue cross-peaks, and thus no further 3D structure determination was attempted on this form. For the *trans* isoform, over 100 of the 184 NOEs were due to interresidue connectivities and thus would be useful in restrained molecular dynamics simulations for 3D structure generation.

In order to ascertain the NOE buildup profile of the *trans* isoform, several cross-peaks were integrated from the NOESY spectra acquired using the mixing times 75, 100, 125, 150, 175, 200, 250, 300, 350, and 400 ms. Buildup rates for some of the cross-peaks are shown in Figure 1. From this graph, it can be concluded that the optimal mixing time for distance calculation is in the 175–200-ms range since the buildup is fairly linear until this time. Since both the 175- and 200-ms spectra gave essentially the same calculated distances, all NOE cross-peaks in the 200-ms mixing time spectrum were integrated and converted to distance restraints to be used in 3D structure determination. It is still likely that spin diffusion is present in the NOEs of this spectrum and may give rise to slight inaccuracies in calculated distances. This is overcome, however, by using three classes of restraints and placing borderline restraints in the wider distance class.

Secondary Structure. A qualitative examination of the NOEs assigned for the *trans* isoform gives an indication of the presence and type of secondary structure that is present in solution. Characteristic NOEs have been identified which are consistent with the presence of two β-turns between residues 134 and 142. These are illustrated in the NOESY spectrum in Figure 2 and the schematic diagram in Figure 3. These NOEs include a $d_{\alpha N}$ $(i,i+2)$ between positions 2 and 4 of the turn and a d_{NN} between positions 3 and 4 of the turn (Chandrasekhar et al., 1991; Wüthrich, 1986). A $d_{\alpha N}$ $(i,i+2)$ is observed between K^{140} and C^{142} of PAK 128–144 *trans* at 4.23 and 8.15 ppm and thus gives substantive evidence that a β-turn is present. This places K^{140} and C^{142} at positions 2 and 4 of the turn and implies that the turn exists between residues 139 and 142. A cross-peak occurring at 8.68 and 8.15 ppm corresponds to the $d_{NN}(3,4)$ NOE which is also characteristic of the β-turn. It is probable that this exists as a type II turn since a very intense $d_{\alpha N}(i,i+1)$ connectivity between K^{140} and G^{141} is observed. For most types of β-turns, a hydrogen bond is present between the carbonyl of residue 1 and the amide proton of residue 4 of the turn. For PAK 128–144, this would be reflected in a lowered temperature coefficient of the C^{142} amide proton (Rose et al., 1985). This is indeed the case as the C^{142} amide has value of 3.0 ppb/K for its temperature coefficient, which is strong indication that this proton is hydrogen-bonded to the carbonyl of P^{139}.

Distinctive connectivities are also observed which indicate the presence of a β-turn between residues 134 and 137 of PAK 128–144. A strong d_{NN} NOE is observed between the amides of Q^{136} and F^{137} at 8.53 and 8.07 ppm. No $d_{\alpha N}(i,i+2)$ is observed between E^{135} and F^{137}; however, this is likely due to overlap with the sequential $d_{\alpha N}(136,137)$ as E^{135} and Q^{136} have very similar α-H chemical shifts. However, $d_{\beta N}(i,i+2)$ NOEs are present between E^{135} and F^{137} at 2.01, 2.12, and 8.07 ppm, thus substantiating the presence of the turn. This would indicate that E^{135} and F^{137} are in positions 2 and 4 of the turn. Since F^{137} is in position 4, it should be involved in

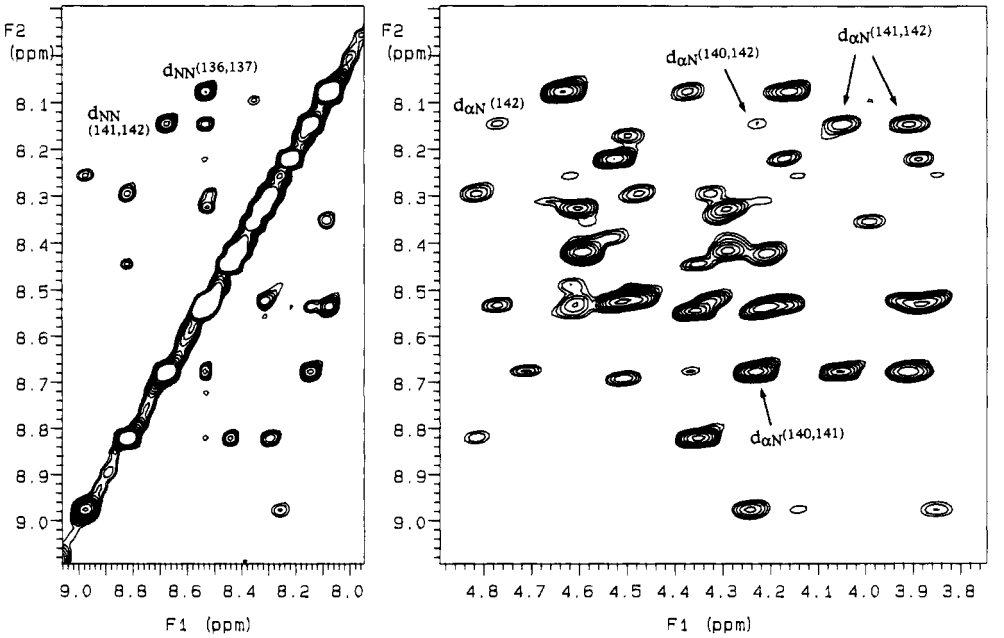

FIGURE 2: d_{NN} and $d_{\alpha N}$ region of the 600-MHz NOESY spectrum of oxidized 5 mM PAK 128–144 in 90% H_2O/10% D_2O (pH 5), 20 mM NaAc, and 100 mM KCl at 5.0 °C. NOEs from residues involved in the turns are labeled.

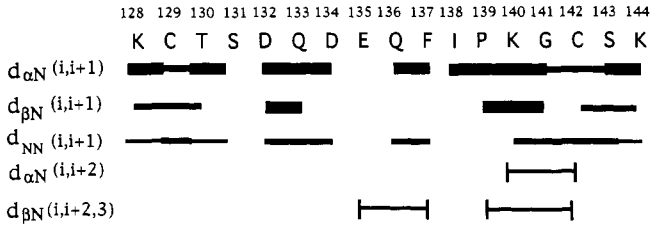

FIGURE 3: Schematic representation of interresidue NOE connectivities from the NOESY spectrum of PAK 128–144. Line thickness indicates the NOE intensity classification of strong, medium, or weak. Lines with bars indicate medium-range NOEs.

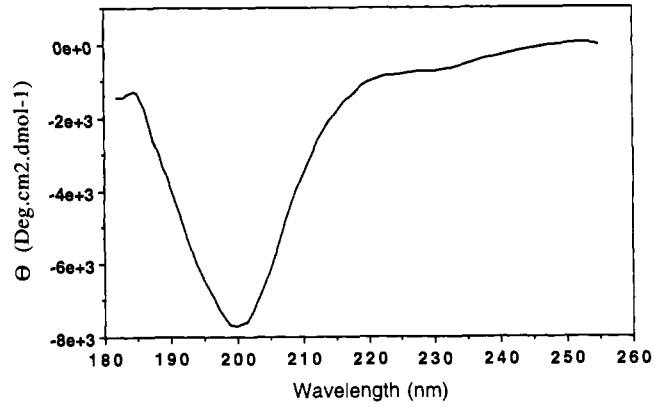

FIGURE 4: Low-ultraviolet CD spectrum of oxidized PAK 128–144 in 0.1 M KCl solution (pH 7.0) at 24.7 °C. Provencher analysis of the spectrum indicated the peptide to be 30% β-turn.

a hydrogen bond. This is shown in the temperature coefficient value of 3.3 ppb/K, demonstrating that the amide proton is involved in a hydrogen bond with the carbonyl of D^{134}. This evidence gives a positive identification of a β-turn between D^{134} and F^{137}. The assignment of the characteristic NOEs in conjunction with the temperature coefficient data demonstrates unequivocally that β-turns are present between residues 134 and 142. CD spectra of PAK 128–144 were taken also to examine the secondary structure as shown in Figure 4. Provencher analysis of the spectra confirmed the presence of β-turns, indicating that approximately 30% of the residues are involved in reverse turns. This analysis also indicated 7% helix, 52% β-sheet, and 11% random coil.

3D Structure Determination. While qualitative analysis of NOE data, in this case, gives a preliminary indication of the type of secondary structure present, it does not provide information on the global fold or on the flexibility of this constrained peptide. In order to determine the 3D structure of PAK 128–144 *trans*, several simulated annealing runs were performed using distance and dihedral restraints. Simulated annealing is appropriate in determining the 3D structures of flexible peptides since it allows for a large sampling of conformational space. High temperature enables the potential energy barrier between local and global minima to be overcome while using lower force constants for all potentials. NOE and dihedral force constants are lowered initially in order to allow greater conformational sampling and then scaled up to satisfy the NOE and dihedral restraints.

A total of 12 SA runs was carried out, with each successive run incorporating a modified restraint file. The initial restraint file consisted of 181 NOE and 14 dihedral restraints and was modified until a set of structures was generated with no significant violations. A summary of the number of restraints per residue is illustrated in Figure 5. In the final run, 25 structures were generated using a restraint file consisting 161 NOE distance, 2 hydrogen bond, and 12 dihedral restraints.

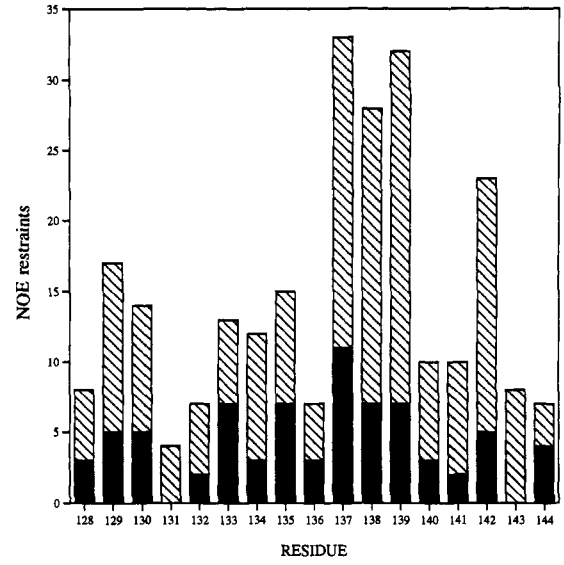

FIGURE 5: Plot of the final number of NOE restraints per residue for PAK 128–144 after 12 simulated annealing runs. The solid bars indicate intraresidue connectivities, while the cross-hatched bars indicate interresidue NOEs.

Twenty NOE distance restraints were removed since they occurred from ambiguous assignments and gave large distance violations in the resulting structures. Two dihedral restraints were removed that were not in allowed regions of ϕ–ψ space. The two hydrogen-bond restraints of the D^{134} carbonyl to the NH of F^{137} and of the P^{139} carbonyl to the amide of C^{142} were added in at runs 9 and 11, respectively, since the β-turns, demonstrated to exist through the NOE patterns and temperature coefficients, were apparent in the structures generated. These restraints were added in order to refine the structures obtained by increasing the number of structures which exhibited the β-turn conformations.

Three-dimensional structural determination of peptides is often complicated by the fact that flexible peptides exist in solution as a large population of interchangeable conformations. Since this interconversion is fast on the NMR time scale, structural information obtained will be the average of these multiple conformations. As a result, 3D structure calculations using NMR data will reflect the conformational averaging and yield a potentially meaningless structure. Attempts have been made to overcome this problem and include the time-average NOE approach (Torda et al., 1989, 1990), NMR-derived multiconformational peptide dynamics (Brüschweiler et al., 1991), and in this laboratory, an averaged relaxation matrix approach (Wang et al., 1993a,b). The latter method searches for the widest range of structures whose calculated averaged NOEs best fit the experimental NOE data.

While conformational averaging undoubtedly plays a role in the 3D structure determination of PAK 128–144, it was not seen as a major obstacle to obtaining meaningful structural information. The constraint of the disulfide bridge allows significantly less conformational flexibility of the peptide as indicated by the average number of NOEs per residue (see Figure 5), which is fairly high at almost 15. Some residues have as many as 30 NOEs per residue. This indicates that a significant population of similarly structured forms is present, at least in the areas of high NOE density. This makes PAK 128–144 amenable to structure determination using simulated annealing with low NOE force constants which, rather than forcing it to a virtual structure that violates geometry, instead violates NOEs and thus samples a range of conformations.

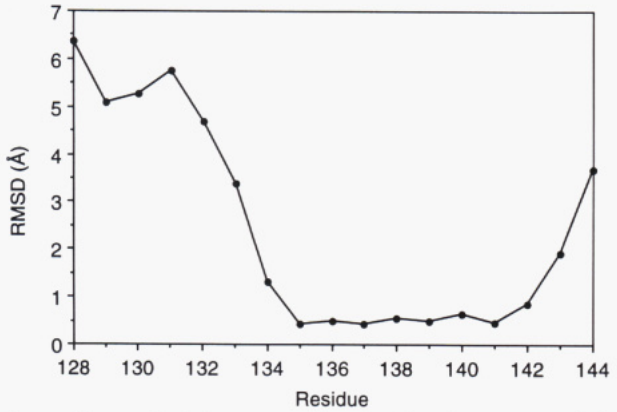

FIGURE 6: rms deviation per residue for the 12 structures of the major class of conformers generated for PAK 128–144 using simulated annealing and superimposed to the average structure.

The SA structures generated mainly serve to examine the secondary structure and flexibility of PAK 128–144. The overall structure shows varying degrees of flexibility in the backbone and side chains and thus is not meaningful in some areas.

For the 25 structures of PAK 128–144 *trans* generated using simulated annealing, a high degree of flexibility is observed in the molecule between residues 128–134 and 142–144. The region from D^{134} to C^{142} shows the highest definition; however, there are three groups of structures observed. One major class is observed with 12 out of the 25 structures showing very similar backbone conformations for the region 134–142. This is illustrated in Figure 6, which shows the rmsd per residue for the 12 structures to the average structure. Between residues 128 and 134 and 143–144, high rmsd's are observed showing that these regions are very flexible. The region encompassed by D^{134}–C^{142} has rmsd values between 1.3 and 0.42, demonstrating that it is considerably less flexible than the rest of the peptide.

All 25 structures show turn conformations between D^{134} and F^{137} and between P^{139} and C^{142}. In the 12 structures of the major class, a type I β-turn encompasses the residues between D^{134} and F^{137}, and a type II turn is found between P^{139} and C^{142}, thus corroborating the evidence afforded by the NOEs diagnostic of the β-turns. For the region 134–140, 23 out of the 25 structures exhibit very similar backbone conformations. The region between D^{134} and K^{140} is significant, as it has been mapped as the epitope for the monoclonal antibody PK99H (Wong et al., 1992). The elucidation of the structure of this region is therefore of importance in the study of antibody–antigen interactions.

DISCUSSION

NMR Solution Structure of PAK 128–144 Trans. Secondary Structure. The ensemble of solution conformations generated for PAK 128–144 *trans* demonstrates the presence of the two β-turns in the region 134–142, as shown in Figure 7. This is significant since it has been proposed that antigenic peptides have a propensity to adopt secondary structure in solution (Dyson et al., 1985, 1988a,b; Chandrasekhar et al., 1991; Zvi et al., 1992; Blumenstein et al., 1992). The two β-turns exist from residues 134 to 137 and from 139 to 142 and have the sequences DEQF and PKGC, respectively. The presence of the two β-turns in the epitope of the monoclonal antibody PK99H is consistent with this theory and with structures of other peptide antigens (Dyson et al., 1985, 1988b; Chandrasekhar et al., 1991; Blumenstein et al., 1992). β-Turns are thus likely to comprise a class of structural motifs for immunogenic regions of peptides and proteins. This conjecture is substantiated by the fact that β-turns constitute greater than 50% of surface-exposed regions in globular proteins (Kuntz, 1972). Since they are surface-exposed, these regions are more likely to be immunogenic, as other types of secondary structure may be buried. This would also explain why peptide fragments of these regions compete with the native protein for antibody binding, as these fragments have a propensity to adopt the same secondary structure as is found in the intact protein. The compact structure of turns is believed to maximize the contact area of the peptide with the antibody surface and allows less conformational restriction than other types of secondary structure (Sherf et al., 1992). This might

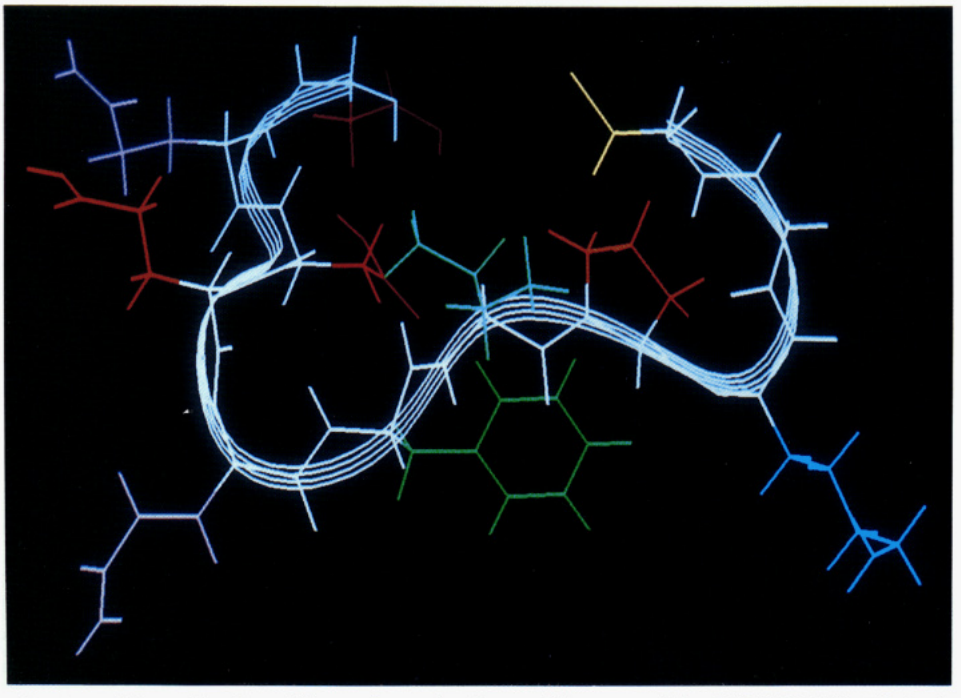

FIGURE 7: Average structure of the major class of the conformational ensemble generated for PAK 128–144 with the backbone represented in ribbon form. The two β-turns can be seen, with the D^{134}–F^{137} turn on the left and the P^{139}–C^{142} turn on the right.

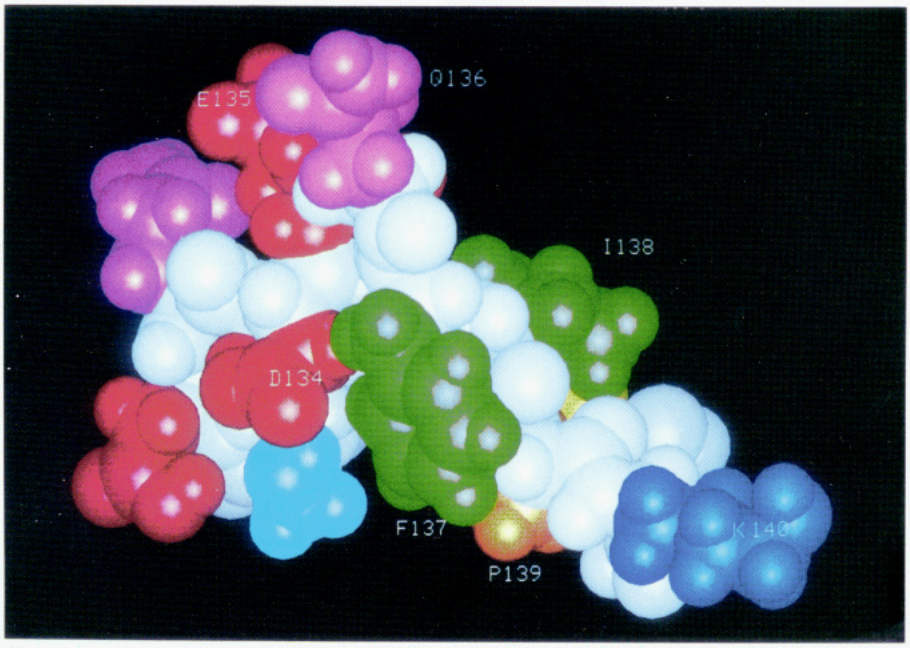

FIGURE 8: CPK representation of the average structure of PAK 128–144 showing the potential binding face for the monoclonal antibody PK99H. Critical residue F^{137}, I^{138}, and K^{140} side chains appear to be directly accessible for antibody binding, while the important residues D^{134} and E^{135} are less so, although still accessible.

be necessary in order for the peptide to fold into the antibody combining site. This hypothesis is predicated in the results of two recent studies of antibody–antigen interactions (Blumenstein et al., 1992; Hinds et al., 1991). These demonstrate that the stabilization of β-turns found in the epitope region of peptide antigens results in increased affinity for their corresponding monoclonal antibody.

Contribution of Peptide Backbone to Antibody Binding. A series of analogs from the C-terminus of the PAK pilin has been used in order to elucidate the nature of the interaction of PAK 128–144 with its monoclonal antibody PK99H (Wong et al., 1992). This investigation showed that the epitope consisted of the seven residues between 134 and 140, i.e., DEQFIPK. Of these residues, F^{137}, I^{138}, and K^{140} were shown to be critical for binding to PK99H, D^{134}, E^{135}, and P^{139} were shown to be important, and Q^{136} was shown to be nonessential for binding, on the basis of a series of single alanine substitutions of PAK 128–144. The 7-residue peptide corresponding to the epitope was demonstrated to bind to PK99H with the same affinity as PAK 128–144 and also showed the same alanine substitution profile as the seven residues in the native peptide. A series of deletion peptides was also studied. The tetrapeptide FIPK, which contains the three critical residues and one important residue, was found not to bind to the antibody significantly; however, when it was extended toward the N-terminus one amino acid at a time, the binding affinity increased markedly. QFIPK bound with a 300-fold lower affinity than native PAK 128–144 and EQFIPK with a 15-fold decrease in binding. The truncation of K^{140} from the heptapeptide also resulted in a large decrease in binding of greater than 10 000-fold.

These data suggest that the type I β-turn, which has been shown to exist in the NMR solution structure of PAK 128–144 between D^{134} and F^{137}, is critical for binding to the antibody, even though these residues individually only lead to relatively small decreases in binding. This can be deduced since FIPK does not bind to PK99H; however, addition of the N-terminal residues substantially increases binding. The importance of the β-turn is also demonstrated, in that PAK 134–140 is tolerant in its binding with the $D^{134}N$ and $E^{135}Q$ substitutions. As substitution of these side chains with alanine, asparagine, and glutamine residues does not significantly change binding, it is conceivable that the β-turn is preserved in these analogs and is thus essential for antibody affinity. The N^{134} substitution is unlikely to disrupt the turn since it is statistically common in position 1 of the type I β-turns found in proteins (Wilmot & Thornton, 1988). It is improbable that the glutamine and alanine substitutions interfere with turn formation since these residues are also commonly found in type I turns.

The decrease in binding affinity that results from the deletion of K^{140} is also noteworthy from an immunological standpoint. Unlike the β-turn that exists between D^{134} and F^{137}, the presence of the β-turn that occurs from P^{139} to C^{142} apparently is not essential for binding to PK99H. Since PAK 134–140 binds with equal affinity as PAK 128–144, the residues G^{141} and C^{142}, which constitute one-half of the type II turn, are obviously not essential for binding. The D^{134}–F^{137} β-turn alone is not sufficient for binding since deletion of K^{140} results in such a marked loss in affinity for PK99H and since the consequence of substitution of the lysine with alanine is a significant decrease in binding. This suggests that the ionic interaction of the lysine side chain is essential for binding and confirms that the P^{139}–C^{142} β-turn is not requisite for binding.

Contribution of Side Chains to Antibody Binding. Examination of the average solution structure of PAK 128–144 *trans* provides further insight into the contribution of side chains of the epitope region due to the high definition of this region in the ensemble. The rest of the average structure may not be meaningful due the high flexibility of these regions. As can be seen from Figure 8, the three critical residues for antibody binding, K^{140}, I^{138}, and F^{137}, appear to be presented on one face of the molecule and thus are accessible to the antibody combining site. P^{139}, which is an important residue for binding, is on the opposite side of this face. It is apparent from the structure and from side chain–side chain NOEs that a hydrophobic interaction occurs between P^{139} and F^{137}, as is observed from the close proximity of the two side chains, and that the aromatic ring of F^{137} is lying parallel to the proline ring. This interaction may be requisite for presentation of the

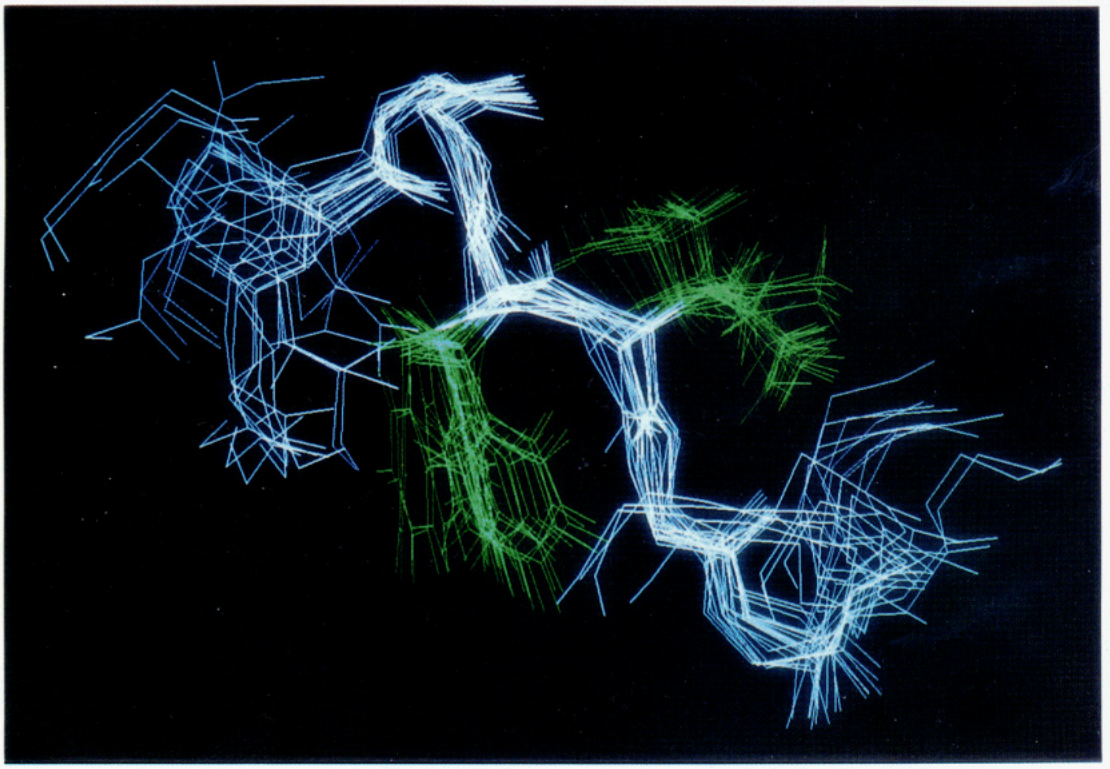

FIGURE 9: Conformational ensemble of the turn structures of PAK 128–144, showing the high definition of the region between residues 134 and 140 and the greater flexibility of the rest of the peptide. The backbone of residues 132–142 and the side chains of F^{137} and I^{138} are displayed.

phenylalanine side chain for binding and thus would explain the decrease in binding when proline is substituted. This suggests that the lower antibody affinity of the P139A analog is a consequence of changes in the conformation of the peptide and that the proline side chain is not necessarily recognized by the antibody. These changes likely result from the lessened hydrophobic interaction, as well as from elimination of the restraint of the cyclic proline ring.

It is also noteworthy that the side chain of Q^{136} appears to lie in the binding interface. It has been demonstrated that Q^{136} can be substituted with smaller amino acids without a significant loss in binding. Introduction of larger side chains, however, i.e., lysine or tyrosine, at this position results in large decreases in the binding affinity of PAK C-terminal peptides (W. Y. Wong, R. T. Irvin, and R. S. Hodges, unpublished results). The presence of Q^{136} in the putative binding interface of PAK 128–144 gives weight to the proposal of Wong et al. (1992), who suggested that Q^{136} is positioned in the binding region but that the side chain has a small contribution to affinity with PK99H. Another observation from the average structure is that the side chains of D^{134} and E^{135} appear to be less accessible for binding, even though they are on the same binding face. As these residues are fairly insensitive to substitution, this suggests that the backbone β-turn conformation makes a larger contribution than the orientation of the side chains. Future experiments to determine the antibody-bound structure of PAK 128–144 should provide the necessary information concerning side-chain presentation and orientation of the peptide backbone in relation to antibody binding. It can be seen that NMR-generated structures of antigenic peptides can be of use in studying antibody–antigen interactions and in postulating a binding interface when the epitope of an antibody is known. It is also possible to observe that certain side chains stabilize the 3D structure of the antigen rather than being directly responsible for antibody binding.

Flexibility of PAK 128–144 Trans in Solution. Consideration of the relationship between the flexibility of antigenic peptides in solution and their recognition by antibodies is salient in the study of antibody–antigen interactions. Crystallographic studies on the immunogenic regions of proteins have shown that continuous epitopes possess higher temperature factors than nonimmunogenic regions (Westhof et al., 1984; Tainer et al., 1984). These results indicate that the regions with greater flexibility are among the most immunogenic in the protein. This is also consistent with the previous conjecture that β-turns are immunogenic, since these are usually surface-exposed and possess a degree of flexibility. It has also been suggested that cross-reactivity of anti-peptide antibodies with the native protein is optimal with regions that are flexible in the intact molecule but have a propensity to adopt secondary structure in the free peptide (Fieser et al., 1987).

The ensemble of NMR solution structures generated for PAK 128–144 *trans* provides an avenue to examine the flexibility of this peptide in solution and relate this to its immunological functioning in a fashion similar to the above-mentioned studies. For the 25 possible conformations produced by the simulated annealing program, reproducibility of the 3D structure using this procedure gives an indication of the variability in the spatial distribution of atoms. The results as shown in Figure 9 demonstrate that the region encompassing D^{134}–K^{140} shows the highest definition in 3D structure and thus is the least flexible. This is demonstrated by the observation that 23 of the 25 structures have essentially the same backbone conformation in this region. This suggests that a high population of conformations exists with the β-turn between D^{134} and F^{137}. G^{141} and C^{142} are more flexible, with 12 of 25 structures showing the same backbone conformation between D^{134} and C^{142}. Examination of the side chains in the structural ensemble provides information on their flexibility. Interestingly, two of the residues that show the least flexibility are F^{137} and I^{138}, which have been demonstrated to be critical for antibody binding. The high definition of these residues is likely due to hydrophobic interactions of these side chains with other parts of the molecule. The side chain of K^{140},

another critical residue, is more flexible; however, this is conceivable due to hydrophilic interactions with the solution. Other side chains in the epitope region appear to be quite flexible, with the exception of P^{139} which due to its cyclic nature is conformationally restricted.

All other regions of the peptide appear to be very flexible, as the backbone and side chains differ markedly in their conformations and have high rmsd values. The apparent rigidity of residues 134–140 is significant as these constitute the epitope region for PK99H. This does not conflict with the previously mentioned crystallographic studies, as PAK 128–144 as a whole is a flexible molecule but contains a nonflexible region. This suggests that the local rigidity within a flexible region of a protein is important for immunogenicity. The rigidity of one sequence within a region with overall flexibility would also explain why the presence of well-defined secondary structure increases the ability of this peptide to compete with the native protein for binding to the monoclonal antibody, as mentioned above (Fieser et al., 1987). This is corroborated by the studies which indicate that stabilization of turns in epitope regions of peptides increases antigen–antibody affinity (Blumenstein et al., 1992; Hinds et al., 1991).

It is also important to consider the mechanism through which antigens bind to antibodies, and the flexibility of PAK 128–144 provides insight into this. Two mechanisms by which antigens bind to antibodies have been proposed. These are (1) the lock and key theory, where the antigen adopts a preferred conformation that is recognized by the antibody and binding occurs, and (2) the induced fit theory, where one part of the molecule binds to the antibody first, and subsequently the rest of the peptide folds into the combining site. The presence of the less flexible secondary structure in PAK 128–144 between residues 134 and 140 seems to corroborate the lock and key theory of antigen binding, since there is less conformational freedom to facilitate folding of the peptide into the antibody combining site. Future work on the antibody-bound structure of PAK 128–144 should yield insight into the mechanism of binding.

CONCLUSIONS

A significant amount of information can be obtained from the ensemble of NMR solution structures generated for PAK 128–144 *trans*. The existence of the type I β-turn in the PK99H epitope validates the theory that antigenic peptides have an innate tendency to adopt a folded conformation in solution. The information obtained from the 3D structure, in conjunction with previous studies on the interaction of PAK 128–144 with PK99H, shows that the β-turn in the epitope region is essential for antibody binding. This also confirms the results of other structural studies of antigenic peptides which report the presence of β-turns. It is thus possible that turns comprise a structural motif of peptide antigens. This may be relevant to the development of synthetic vaccines, as through the use of constrained peptides, it may be beneficial to lock in a particular turn conformation of the peptide and thus improve its immunogenicity.

The structures also suggest a plausible binding interface of the peptide in which the essential residues might be presented to the antibody combining site and suggest that some residues important for antibody binding stabilize the peptide conformation rather than interacting directly with the antibody itself.

The conformational ensemble also provides information on the flexibility of PAK 128–144 in solution and indicates that the least flexible regions of the peptide constitute the epitope of the monoclonal antibody PK99H. This suggests that local rigidity within an overall flexible loop is important in immunogenicity. Since the least flexible region is involved in antibody binding, it is feasible that this region is also involved in interaction with the host cell receptor of the *P. aeruginosa* pilus.

ACKNOWLEDGMENT

We thank Paul Semchuk for peptide synthesis, purification, and mass spectrometry, Kim Oikawa for CD spectroscopy, Robert Boyko and Tim Jellard for computer programming assistance, and Dr. Jianjun Wang for helpful discussions.

REFERENCES

Bax, A., & Davis, D. G. (1985) *J. Magn. Reson. 65*, 355–360.
Blumenstein, M., Matsueda, G. R., Timmons, S., & Hawiger, J. (1992) *Biochemistry 31*, 10692–10698.
Brüschweiler, R., Blackledge, M., & Ernst, R. R. (1991) *J. Biol. NMR 1*, 3–11.
Chandrasekhar, K., Profy, A. T., & Dyson, H. J. (1991) *Biochemistry 30*, 9187–9194.
Doig, P., Sastry, P. A., Hodges, R. S., Lee, K. K., Paranchych, W., & Irvin, R. T. (1990) *Infect. Immunol. 58*, 124–130.
Dyson, H. J., Cross, K. J., Houghten, R. A., Wilson, I. A., Wright, P. E., & Lerner, R. A. (1985) *Nature 318*, 480–483.
Dyson, H. J., Rance, M., Houghten, R. A., Lerner, R. A., & Wright, P. E. (1988a) *J. Mol. Biol. 201*, 161–200.
Dyson, H. J., Rance, M., Houghten, R. A., Wright, P. E., & Lerner, R. A. (1988b) *J. Mol. Biol. 201*, 201–217.
Fieser, T. M., Tainer, J. A., Geysen, H. M., Houghten, R. A., & Lerner, R. A. (1987) *Proc. Natl. Acad. Sci. U.S.A. 84*, 8568–8572.
Hinds, H. G., Welsh, J. H., Brennand, D. M., Fisher, J., Glennie, M. J., Richards, H. G. J., Turner, D. L., & Robinson, J. A. (1991) *J. Med. Chem. 34*, 1777–1789.
Irvin, R. T. (1993) *Pseudomonas aeruginosa* as an opportunistic pathogen (Campa, M., Ed.) Plenum Press, New York.
Irvin, R. T., Doig, P., Lee, K. K., Sastry, P. A., Paranchych, W., Todd, T., & Hodges, R. S. (1989) *Infect. Immunol. 57*, 3720–3726.
Irvin, R. T., Doig, P., Sastry, P. A., Heller, B., & Paranchych, W. (1990) *Microb. Ecol. Health Dis. 3*, 39–47.
Jeener, J., Meier, B. H., Bachmann, P., & Ernst, R. R. (1979) *J. Chem. Phys. 71*, 4546–4553.
Kuntz, I. D. (1972) *J. Am. Chem. Soc. 94*, 4009–4012.
Lee, K. K., Paranchych, W., & Hodges, R. S. (1990) *Infect. Immunol. 58*, 2727–2732.
McInnes, C., Kay, C. M., Hodges. R. S., & Sykes, B. D. (1993) *Biopolymers* (in press).
Nilges, M., Clore, G. M., & Gronenborn, A. M. (1988) *FEBS Lett. 229*, 317–324.
Nilges, M., Clore, G. M., & Gronenborn, A. M. (1990) *Biopolymers 29*, 813–822.
Paranchych, W., Sastry, P. A., Volpel, K., Loh, B. A., & Speert, D. P. (1986) *Clin. Invest. Med. 9*, 113–118.
Paranchych, W., Pasloske, B. L., & Sastry, P. A. (1990) in *Pseudomonas:* Biotransformations, Pathogenesis and Evolving Biotechnology (Sliver, S., Chakrabarty, A. M., Iglewski, B. B. H., & Kaplan, S., Eds.) pp 342–351, American Society for Microbiology, Washington, D.C.
Paranchych, W., Glasier, L. M. G., Ellert, N. W., Lane-Bell, P. M., Lee, K. K., Hodges, R. S., & Irvin, R. T. (1993) *Anim. Sci. Res.* (submitted for publication).
Pasloske, B. L., Sastry, P. A., Finlay, B. B., & Paranchych, W. (1988) *J. Bacteriol. 170*, 3738–3741.
Piantini, U., Sorensen, O. W., & Ernst, R. R. (1982) *J. Am. Chem. Soc. 104*, 6800–6801.
Pier, G. B. (1985) *J. Infect. Dis. 151*, 575–580.

Provencher, S. W., & Glöckner J. (1981) *Biochemistry 20*, 33–37.
Ramphal, R., Sadoff, J. C., Pyle, M., & Silipigni, J. D. (1984) *Infect. Immunol. 44*, 38–40.
Rivera, M., & Nicotra, M. B. (1982) *Am. Rev. Respir. Dis. 126*, 833–836.
Rose, G. D., Gierasch, L. M., & Smith, J. A. (1985) *Adv. Protein Chem. 37*, 1–107.
Sherf, T., Hiller, R., Naider, F., Levitt, M., & Anglister, J. (1992) *Biochemistry 31*, 6884–6897.
Stanfield, R. L., Fieser, T. M., Lerner, R. A., & Wilson, I. A. (1990) *Science 248*, 712–719.
States, D. J., Haberkorn, R. A., & Ruben, D. J. (1982) *J. Magn. Reson. 48*, 286–292.
Tainer, J. A., Getzoff, E. D., Alexander, H., Houghten, R. A., Olson, A. J., & Lerner, R. A. (1984) *Nature 312*, 127–134.
Torda, A. E., Scheek, R. M., & Van Gunsternen, W. F. (1989) *Chem. Phys. Lett. 157*, 289–294.
Torda, A. E., Scheek, R. M., & Van Gunsternen, W. F. (1990) *J. Mol. Biol. 214*, 223–235.
Wang, J., Sönnichsen, F. D., Boyko, R., Hodges, R. S., & Sykes, B. D. (1993a) *Techniques in Protein Chemistry IV*, pp 569–575, Academic Press, Inc., San Diego, CA.
Wang, J., Hodges, R. S., & Sykes, B. D. (1993b) *Proc. 13th Am. Pept. Symp.* (in press).
Westhof, E., Altschuh, D., Moras, D., Bloomer, A. C., Mondragon, A., Klug, A., & Van Regenmortel, M. H. V. (1984) *Nature 311*, 123–126.
Wilmot, C. M., & Thornton, J. M. (1988) *J. Mol. Biol. 203*, 221–232.
Wong, W. Y., Irvin, R. T., Paranchych, W., & Hodges, R. S. (1992) *Protein Sci. 1*, 1308–1318.
Wüthrich, K. (1986) *NMR of Proteins and Nucleic Acids*, John Wiley and Sons, New York.
Zvi, A., Hiller, R., & Anglister, J. (1992) *Biochemistry 31*, 6972–6979.